

Rashba Spin-Orbit Coupling Induced Topological Phases Transition in Honeycomb Nanoribbon Heterojunction

Hao-Ru Wu, Jhih-Shih You*, Yiing-Rei Chen*, and Hong-Yi Chen*

Department of Physics, National Taiwan Normal University, Taipei, 116, Taiwan

(Revised 23 February 2026)

We explore the emergence of non-trivial topological phases arising from the interplay between structural geometry and the spin degree of freedom. Our system is a honeycomb nanoribbon heterostructure with armchair edges, consisting of a central Rashba spin-orbit coupled (SOC) region sandwiched between two pristine armchair nanoribbons. As the strength of Rashba SOC is increased, topological edge states exhibit at the interface between the Rashba SOC and pristine armchair honeycomb nanoribbon (ANR), and these edge states remain robust under edge perturbations. In addition, we find that for a finite width ANR, Rashba SOC can open/close a gap depending on its strength, which leads to a topological phase transition. This work provides an alternative perspective on how Rashba SOC influences topological properties.

Symmetry plays a central role in connecting topological characteristics and electronic properties in quantum systems. Due to the bulk-edge correspondence, the underlying symmetries dictate that the number of symmetry-protected edge modes emerge from a given topological phase. In one-dimensional systems, this correspondence is classified by the Altland-Zirnbauer symmetry classes, known as the ten-fold way [1-3]. Notably, recent studies have revealed additional topological phases induced by structural geometries. A quantized Zak phase can arise in quasi-one-dimensional systems with distinct intercell hopping that breaks inversion symmetry [4]. Moreover, graphene-based systems with nontrivial structural geometry and chiral symmetry can host symmetry-protected edge modes [5, 6]. Motivated by these findings, we investigate the emergence of edge modes in a system featuring nontrivial structural geometry and broken inversion symmetry.

Recently, the role of symmetry in topological phases has been widely discussed. On one hand, the topology in asymmetry system have been investigated [4,7-10]. For one-dimensional systems with no symmetry beyond translation, a more general topological invariant has been proposed to establish the bulk-edge correspondence [7, 9]. In addition, ferromagnetic edge states have been discovered in asymmetric Janus graphene nanoribbon [10]. On the other hand, the topological classification and edge properties of symmetric system has also been studied [5, 6]. For an armchair graphene nanoribbon (GNR), which is chiral symmetric, the topological invariant is developed to classify the different ribbon widths and spatial symmetries. For example, a junction between a 9-armchair GNR (9-AGNR) and a 13-armchair GNR (13-AGNR) junction supports symmetry-protected edge states at its zigzag boundary. These discoveries have inspired numerous approaches to

engineer topological phases in nanoribbons, including edge-shape modifications [10-12], graphene antidot superlattices [13], strain engineering [14], and the application of in-plane electric fields [15, 16].

Here, we focus on system that break inversion symmetry through Rashba spin-orbit coupling (SOC), which typically induced by an external electric field from a substrate [17] or a gate voltage [18]. Rashba SOC is widely applied to graphene system involving spin transport and spintronics, as its strength can significantly exceed intrinsic SOC via substrate proximity effects, electric fields, or heterostructure engineering [19-21]. In addition, equilibrium spin current has been studied in graphene nanoribbon (GNR) heterostructure formed by pristine GNR and Rashba SOC GNR [22].

We investigate the topological properties of a honeycomb-lattice heterostructure in which Rashba SOC serves as the sole tunable parameter controlling the topological phase. Specifically, we consider an armchair nanoribbon with Rashba SOC (RANR) embedded between two pristine armchair nanoribbons (PANRs), forming a PANR-RANR-PANR (PRP) junction. By varying the Rashba SOC strength, the RANR undergoes topological phase transitions that yield distinct topological classes. According to the bulk-edge correspondence, interfaces between PANR and RANR regions with different topological invariants host localized topological edge modes.

Such a heterostructure can be implemented in photonic crystal systems. Photonic analogues of Rashba SOC have recently been observed [23-26], where the helicity of light polarization mimics the electronic spin degree of freedom. Moreover, photonic crystals can be fabricated into heterostructures [26] with armchair- or zigzag-type nanoribbon geometries [27, 28]. This

photonic platform enables precise control of the effective Rashba SOC and offer a versatile route for realizing and manipulating a variety of topological phases.

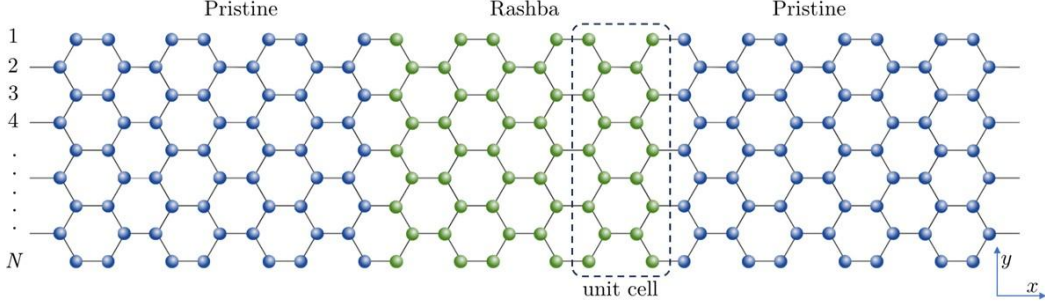


FIG. 1. (Color online) The PANR-RANR-PANR heterostructure. Only the hopping between two green atomic sites contains Rashba SOC.

We consider a heterojunction of three armchair honeycomb nanoribbons of the width N as illustrated in Fig. 1. The Hamiltonian of the PANR-RANR-PANR (PRP) heterostructure is

$$\hat{H} = \sum_{\langle i,j \rangle} \sum_{\alpha} t_0 \hat{c}_{i\alpha}^{\dagger} \hat{c}_{j\alpha} + \sum_{\langle i,j \rangle \in \text{RGNR}} \sum_{\alpha\beta} i t_R \hat{c}_{i\alpha}^{\dagger} \mathbf{z} \cdot (\boldsymbol{\sigma}_{\alpha\beta} \times \boldsymbol{\delta}_{ij}) c_{j\beta} + \text{h. c.},$$

where $\langle i,j \rangle$ includes all configurations of the nearest-neighbor sites, α and β are the spin indices, $c_{i\alpha}^{\dagger}$ ($c_{i\alpha}$) is the creation (annihilation) operator with spin α at site i , t_0 is the nearest-neighbor hopping strength, t_R is the Rashba SOC strength, $\boldsymbol{\sigma}$ are the Pauli matrices, and $\boldsymbol{\delta}_{ij}$ is the unit vector pointing in the direction from site i to site j . Hereafter, we set the nearest-neighbor hopping strength as the unit of energy, $t_0 = 1$. Also, we apply periodic boundary condition on the ends of the pristine armchair nanoribbon to prevent the possible edge states on the rightmost and leftmost zigzag edges.

For $t_R = 0$, the PRP heterostructure reduces to a pristine armchair nanoribbon. The pristine armchair nanoribbon is gapped unless the width N of the armchair nanoribbon satisfy the condition $N = 3M - 1$ with an integer $M > 0$ [29]. Previous studies have shown analytically that the band gap closes every three ribbon widths [30, 31]. For armchair nanoribbon, the edge boundary condition discretizes the wavenumber in the y -direction. When the allowed wavenumber hit the Dirac points, which corresponds to the width $N = 3M - 1$, then the nanoribbon becomes metallic [31]. Hence, for $N = 2, 5, 8, 11$, and so on, the armchair nanoribbon is gapless.

Notably, the additional midgap states emerge within the gap as t_R exceeds a certain number. Fig. 2 shows the energy spectrum and the density of states for the case

$N = 6$, for different values of t_R . In stark contrast to Fig. 2(a) for $t_R = 0.4$, Fig. 2(c) for $t_R = 0.8$ clearly shows the existence of four midgap states, which are two-fold spin degeneracy at energies 0^+ and 0^- . This leads to the pronounced peak at the vicinity of $E = 0$ in the density of state shown in Fig. 2(d).

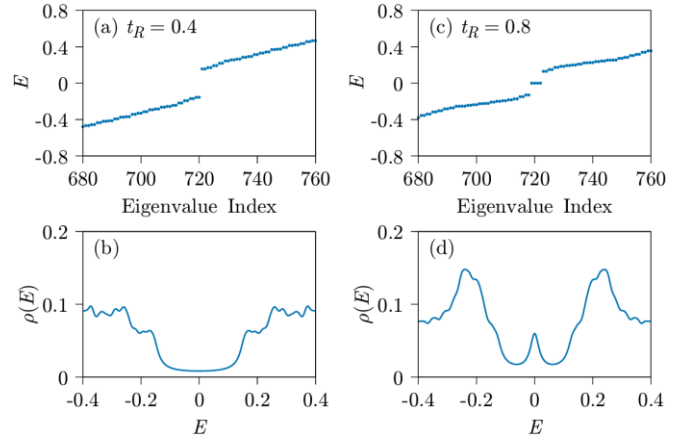


FIG. 2. (a)(c) Energy levels for $N = 6$ heterostructure armchair nanoribbon with $t_R = 0.4$ and 0.8 . The energy gap is 0.26 , 0.31 respectively. (b)(d) The density of state for $t_R = 0.4$ and 0.8 .

We further explore the local density map for the heterostructure in Fig. 3(a), obtained by integrating the distribution of all mid-gap states. The local density at each point is given by summing the spin-up and spin-down probabilities. We found that these mid-gap states are exponentially localized at the interface between PANR and RANR. In addition, for different interfaces, such as zigzag (Fig. 3(b)) and bearded (Fig. 3(c)), we can also observe the existence of four midgap edge states. This remarkable robustness to a variety of interfaces suggests that these states have a topological origin.

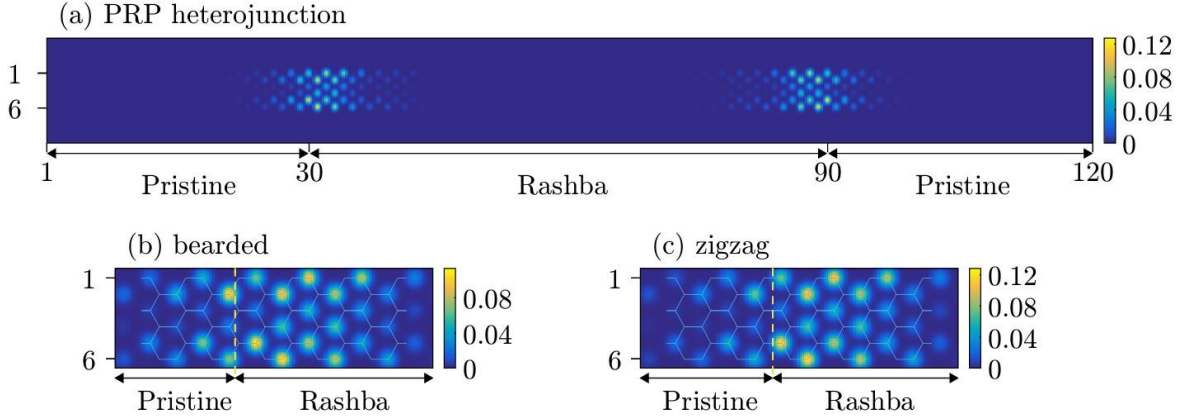


FIG. 3. (Color online) (a). The spatial probability distribution of all midgap states for $N = 6$ and $t_R = 0.8$. (b-c). Distribution plot for different type of interfaces between pristine and Rashba segments.

To understand the topology of the system, we now consider an infinite armchair nanoribbon with width N [5], whose unit cell is a piece containing $2N$ atomic sites, as shown in Fig. 1. Due to the translational symmetry along the direction parallel to the edges, the Bloch momentum k is a good quantum number and the Hamiltonian of the quasi-1-D system can be written in a fully block-off-diagonal matrix

$$\mathcal{H} = \begin{pmatrix} 0 & h_k^\dagger \\ h_k & 0 \end{pmatrix}$$

in the basis $\{|A_1^\dagger\rangle, \dots, |A_N^\dagger\rangle, |B_1^\dagger\rangle, \dots, |B_N^\dagger\rangle\}$, where A and B denote the sublattice and h_k is a $2N \times 2N$ matrix. Since the Hamiltonian preserves chiral (sublattice) symmetry, its 1-D topological properties can be characterized by the winding number [32]

$$W = \int_{-\pi}^{\pi} \frac{dk}{2\pi i} \text{Tr}[h_k^{-1} \partial_k h_k] = \int_{-\pi}^{\pi} \frac{dk}{2\pi i} \partial_k \log[\text{Det}(h_k)].$$

The winding number equals to the number of times the trajectory of $\det(h_k)$ winds around the origin in the complex plane.

For $N = 6$, in the absence of Rashba SOC, the bulk armchair nanoribbon exhibits a finite energy gap (Fig. 4(a)). The trajectory of $\text{Det}(h_k)$ in the complex plane encircles the origin twice, corresponding to a winding number $W = 2$ (Fig. 4(d)). As the Rashba SOC strength t_R increases, the gap gradually decreases. At $t_R = 0.624$, the gap closes (Fig. 4(b)), and the trajectory of $\text{Det}(h_k)$ touches the origin, rendering the winding number ill-defined (Fig. 4(e)). Upon further increasing t_R , the gap reopens (Fig. 4(c)), and the trajectory of $\text{Det}(h_k)$ encloses the origin four times, yielding a winding number $W = 4$ (Fig. 4(f)). These results demonstrate that Rashba SOC drives a topological phase

transition in armchair nanoribbon, characterized by a change in winding number from $W = 2$ to $W = 4$.

We note that when the z -axis values are obtained from the periodic function $\sin(k)$, the winding number can be interpreted as a two-dimensional projection of a three-dimensional unknot trajectory, represented by the red curves in Figs. 4(d)–4(f). For $t_R = 0$, the corresponding three-dimensional curve forms a torus knot $\mathcal{T}(3,1)$, where the trajectory winds three times around the torus hole and once around the tube.

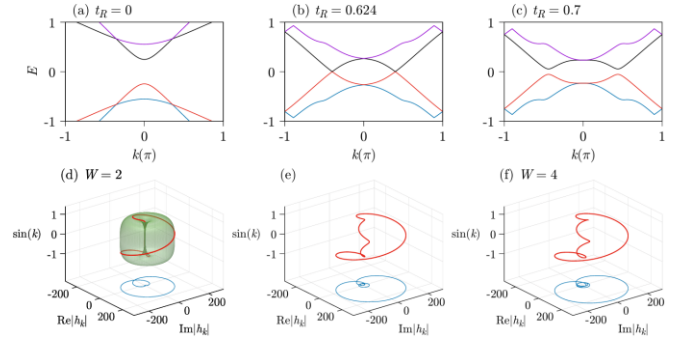


FIG. 4. (Color online) (a) – (c) Four energy bands nearest to the Fermi level with $t_R = 0, 0.624$ and 0.7 . In x axis, k are in units of π . (d) – (f) The path of determinant of h_k in the complex plane as k travels through the whole Brillouin zone with $t_R = 0, 0.624$ and 0.7 . The number of times h_k path includes origin point corresponds to the winding number W .

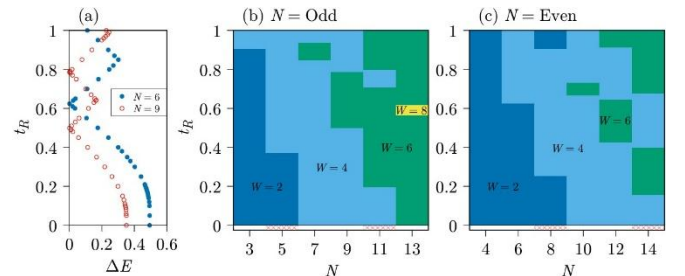


FIG. 5. (Color online) The winding number phase diagram for Rashba SOC strength t_R and the width N , for N is (a) odd and (b) even numbers. Regions printed in different colors represent different winding number, and slash area corresponds to a gapless armchair nanoribbon. The phases transition occurred for $N = 3M - 1$, and it's only valid for small t_R .

In Fig. 5(a), we show the energy gap versus the Rashba SOC strength t_R for $N \neq 3M - 1$ nanoribbons. When increasing the Rashba SOC strength, the energy gap quadratically decreases at small t_R . For $t_R \neq 0$, new Dirac points appear at the vicinity of the original Dirac points with the distances $\sim t_R^2$ for small strength of t_R [33]. As increase t_R , the allowed wavenumbers in the y -direction moves close to the new Dirac points, the size of gap decreases quadratically. As a consequence, we obtain a quadratically relation of the gap versus the Rashba strength.

Fig. 5(b) and 5(c) show the topological phase diagram as a function of the armchair nanoribbon width N and Rashba SOC strength t_R . When $t_R = 0$, our winding number calculations are consistent with the topological index, known as the chiral phase index (CPI) [6]. Upon turning on Rashba SOC, the originally gapless nanoribbons with $N = 2, 5, 8, 11, 14$ become gapped and possess a nontrivial winding number. Moreover, when increasing t_R , the winding number changes only by two at each transition. For instance, the winding number for $N = 6$ is equal to 2 when $t_R = 0.4$ and becomes 4 when $t_R = 0.8$.

In the PRP heterostructure, the pristine and Rashba regions share the same width but are characterized by different winding numbers due to the presence or absence of Rashba spin-orbit coupling. For example, as $N = 6$, the winding number in the pristine region is $W = 2$. By tuning the strength of Rashba SOC t_R on the embedded region, the winding number can change from $W = 2$ to $W = 4$. Thus, the difference of winding number between two regions gives rise to the boundary states localized at the interface (shown in Fig. 2). According to bulk-edge correspondences, this winding number difference leads to the emergence of four symmetry-protected edge states (shown in Figs. 3).

In conclusion, we have studied the PANR-RANR-PANR (PRP) heterostructure. We find that the topological edge states can be induced by increasing Rashba SOC and verify the topological edge states exist as PANR and RANR have different winding numbers. When the difference of winding numbers is larger than zero, the topological edge states emerge at the interface between PANR and RANR. We also found that for a given value of N , the topological phase transition can occur by tuning the value of Rashba SOC t_R . Our work explores topological phases that arises from the interplay between nanoribbon geometry and Rashba spin-orbit coupling. Unlike previous studies, where topological edge states were generated by composing nanoribbons of different geometries, our findings demonstrate topological edge states can emerge within a single nanoribbon geometry. Moreover, this mechanism may not be limited to the honeycomb lattice and can be extended to other bipartite lattice systems to effectively generate topological edge states.

In Kane-Mele model on graphene [34, 35], the intrinsic SOC opens a band gap at the Dirac points of two-dimensional (2D) hexagonal lattices and drive the system into topological quantum spin Hall (QSH) states. In contrast, Rashba SOC closes intrinsic-SOC-induced band gap and transform the system from a QSH phase into a trivial, gapless spin-split metallic state [36–38]. In our nanoribbon system, however, Rashba SOC opens nanoribbon's band gap and produces additional topological edge states when increasing Rashba SOC strength. Our work discovers a new identity for Rashba SOC in graphene-like system.

ACKNOWLEDGMENTS

We thank Ion Cosma Fulga for useful discussion. The authors would like to thank ‘‘Higher Education Sprout Project’’ of National Taiwan Normal University and the Ministry of Education (MOE), Taiwan. J.-S.Y. acknowledges support from the National Science and Technology Council (NSTC), Taiwan, under Grant No. NSTC 113-2112-M-003-015, and from TG 3.2 of NCTS at NTU. Y.-R.C thanks the support from National Science and Technology Council (NSTC), grant No. NSTC 114-2635-M-003-001-MY3.

*Author to whom all correspondence should be addressed:

jhihshihyou@ntnu.edu.tw
yrchen@phy.ntnu.edu.tw
hongyi@ntnu.edu.tw

[1] Ching-Kai Chiu, Jeffrey C. Y. Teo, Andreas P. Schnyder, and Shinsei Ryu, Classification of topological quantum matter with symmetries, Rev. Mod. Phys. 88, 035005 (2016).

- [2] Alexei Kitaev, Periodic table for topological insulators and superconductors, *AIP Conf. Proc.* 1134, 22 (2009).
- [3] Shinsei Ryu, Andreas P Schnyder, Akira Furusaki, and Andreas W.W. Ludwig, Topological insulators and superconductors: Tenfold way and dimensional hierarchy, *New J. Phys.* 12, 065010 (2010).
- [4] Yi-Xin Xiao, Guancong Ma, Zhao-Qing Zhang, and C. T. Chan, Topological Subspace-Induced Bound State in the Continuum, *Phys. Rev. Lett.* 118, 166803 (2017).
- [5] Ting Cao, Fangzhou Zhao, and Steven G. Louie, Topological Phases in Graphene Nanoribbons: Junction States, Spin Centers, and Quantum Spin Chains, *Phys. Rev. Lett.* 119, 076401 (2017).
- [6] Jingwei Jiang and Steven G. Louie, Topology Classification using Chiral Symmetry and Spin Correlations in Graphene Nanoribbons, *Nano Lett.* 2021, 21, 1, 197–202.
- [7] Janet Zhong, Heming Wang, Alexander N. Poddubny, and Shanhui Fan, Topological Nature of Edge States for One-Dimensional Systems without Symmetry Protection, *Phys. Rev. Lett.* 135, 016601 (2025).
- [8] H. C. Wu and L. Jin, Topological zero modes from the interplay of PT symmetry and anti-PT symmetry, *Phys. Rev. B* 112, 125146 (2025).
- [9] Yunlin Li, Yufu Liu, Xuezhi Wang, Haoran Zhang, Xunya Jiang, Nontrivial topology in one- and two-dimensional asymmetric systems with chiral boundary states, *arXiv:2509.20834*.
- [10] Shaotang Song, Yu Teng, Weichen Tang, Zhen Xu, Yuanyuan He, Jiawei Ruan, Takahiro Kojima, Wenping Hu, Franz J. Giessibl, Hiroshi Sakaguchi, Steven G. Louie & Jiong Lu, Janus graphene nanoribbons with localized states on a single zigzag edge, *Nature* 637, 580–586 (2025).
- [11] Kuan-Sen Lin, and Mei-Yin Chou, Topological Properties of Gapped Graphene Nanoribbons with Spatial Symmetries, *Nano Lett.* 2018, 18, 11, 7254–7260.
- [12] Yea-Lee Lee, Fangzhou Zhao, Ting Cao, Jisoon Ihm, Steven G. Louie, Topological Phases in Cove-Edged and Chevron Graphene Nanoribbons: Geometric Structures, \mathbb{Z}_2 Invariants, and Junction States, *Nano Lett.* 2018, 18, 11, 7247–7253.
- [13] Jianing Wang, Weiwei Chen, Zhengya Wang, Jie Meng, Ruoting Yin, Miaogen Chen, Shijing Tan, Chuanxu Ma, Qunxiang Li, and Bing Wang, Designer topological flat bands in one-dimensional armchair graphene antidot lattices, *Phys. Rev. B* 110, 115138 (2024).
- [14] Anhua Huang, Shasha Ke, Ji-Huan Guan, Jun Li, and Wen-Kai Lou, Strain-induced topological phase transition in graphene nanoribbons, *Phys. Rev. B* 109, 045408 (2024).
- [15] Fangzhou Zhao, Ting Cao, and Steven G. Louie, Topological Phases in Graphene Nanoribbons Tuned by Electric Fields, *Phys. Rev. Lett.* 127, 166401 (2021).
- [16] David M T Kuo, Topological states in finite graphene nanoribbons tuned by electric fields, *J. Phys.: Condens. Matter* 37, 085304 (2025).
- [17] A. Varykhalov, J. Sánchez-Barriga, A. M. Shikin, C. Biswas, E. Vescovo, A. Rybkin, D. Marchenko, and O. Rader, Electronic and Magnetic Properties of Quasifreestanding Graphene on Ni, *Phys. Rev. Lett.* 101, 157601 (2008).
- [18] Y. A. Bychkov and E. I. Rashba, Properties of a 2D Electron Gas with Lifted Spectral Degeneracy, *JETP Lett.* 39, 78-83 (1984).
- [19] Bowen Yang, Mark Lohmann, David Barroso, Ingrid Liao, Zhisheng Lin, Yawen Liu, Ludwig Bartels, Kenji Watanabe, Takashi Taniguchi, and Jing Shi, Strong electron-hole symmetric Rashba spin-orbit coupling in graphene/monolayer transition metal dichalcogenide heterostructures, *Phys. Rev. B* 96, 041409(R) (2017).
- [20] M. Ingot, V. K. Dugaev, A. Dyrdał, and J. Barnaś, Graphene with Rashba spin-orbit interaction and coupling to a magnetic layer: Electron states localized at the domain wall, *Phys. Rev. B* 104, 214408 (2021).
- [21] A. Poszwa, Spin orbit coupling effect on coherent transport properties of graphene nanoscopic rings in external magnetic field, *Scientific Reports* 14, 31554 (2024).
- [22] Huan Zhang, Zhongshui Ma & Jun-Feng Liu, Equilibrium spin current in graphene with Rashba spin-orbit coupling, *Scientific Reports*, 4, 6464 (2014).
- [23] Aditya Tripathi, Anastasiia Zalogina, Jiayan Liao, Matthias Wurdack, Eliezer Estrecho, Jiajia Zhou, Dayong Jin, Sergey S. Kruk, and Yuri Kivshar, Metasurface-Controlled Photonic Rashba Effect for Upconversion Photoluminescence. *Nano Lett.* 2023, 23, 6, 2228–2232.
- [24] Jingyi Tian, Giorgio Adamo, Hailong Liu, Maciej Klein, Song Han, Hong Liu, and Cesare Soci, Optical Rashba Effect in a Light-Emitting

- Perovskite Metasurface, *Advanced Materials* 34, 2109157 (2022).
- [25] N. Shitrit, Igor Yulevich, Elhanan Maguid, Dror Ozeri, Dekel Veksler, Vladimir Kleiner, and Erez Hasman, Spin-Optical Metamaterial Route to Spin-Controlled Photonics. *Science*, 340, 724-726 (2013).
- [26] Kexiu Rong, Bo Wang, Avi Reuven, Elhanan Maguid, Bar Cohn, Vladimir Kleiner, Shaul Katznelson, Elad Koren & Erez Hasman, Photonic Rashba effect from quantum emitters mediated by a Berry-phase defective photonic crystal. *Nature Nanotechnology*, 15, 927-933 (2020).
- [27] Qi Zhong, Yongsheng Liang, Shiqi Xia, Daohong Song, and Zhiang Chen, Observation of Topological Armchair Edge States in Photonic Biphenylene Network. *Advanced Optical Materials*, 13, 2500152 (2025).
- [28] Shiqi Xia, Yongsheng Liang, Liqin Tang, Daohong Song, Jingjun Xu, and Zhigang Chen, Photonic Realization of a Generic Type of Graphene Edge States Exhibiting Topological Flat Band. *Phys. Rev. Lett.* 131, 013804 (2023).
- [29] Kyoto Nakada, Mitsutaka Fujita, Gene Dresselhaus, and Mildred S. Dresselhaus, Edge state in graphene ribbons: Nanometer size effect and edge shape dependence. *Phys. Rev. B* 54, 17954 (1996).
- [30] L. Brey, and H. A. Fertig, Electronic states of graphene nanoribbons studied with the Dirac equation, *Phys. Rev. B* 73, 235411 (2006).
- [31] Katsunori Wakabayashi, Ken-ichi Sasaki, Takeshi Nakanishi and Toshiaki Enoki, Electronic states of graphene nanoribbons and analytical solutions. *Sci. Technol. Adv. Mater.* 11, 054504 (2010).
- [32] Maria Maffei, Alexandre Dauphin, Filippo Cardano, Maciej Lewenstein and Pietro Massignan, Topological characterization of chiral models through their long-time dynamics. *New J. Phys.* 20, 013023 (2018).
- [33] Mahdi Zarea and Nancy Sandler, Rashba spin-orbit interaction in graphene and zigzag nanoribbons. *Phys. Rev. B* 79, 165442 (2009).
- [34] C. L. Kane and E. J. Mele, Quantum Spin Hall Effect in Graphene, *Phys. Rev. Lett.* 95, 226801 (2005).
- [35] C. L. Kane and E. J. Mele, Z₂ Topological Order and the Quantum Spin Hall Effect, *Phys. Rev. Lett.* 95, 146802 (2005).
- [36] Kh. Shakouri, M. Ramezani Masir, A. Jellal, E. B. Choubabi, and F. M. Peeters, Effect of spin-orbit couplings in graphene with and without potential modulation, *Phys. Rev. B* 88, 115408 (2013).
- [37] L. Sheng, D. N. Sheng, C. S. Ting, and F. D. M. Haldane, Nondissipative Spin Hall Effect via Quantized Edge Transport, *Phys. Rev. Lett.* 95, 136602 (2005).
- [38] D. N. Sheng, Z. Y. Weng, L. Sheng, and F. D. M. Haldane, Quantum Spin-Hall Effect and Topologically Invariant Chern Numbers, *Phys. Rev. Lett.* 97, 036808 (2006).